

Estimation of Backing Influence on Halftone Reflectance

Matthias Scheller Lichtenauer (1), Hanno Hoffstadt (2), Andreas Kraushaar (3), Berthold Oberhollenzer (3), Peter Zolliker (1); (1) EMPA, Duebendorf, Switzerland, (2) GMG GmbH & Co. KG, Tuebingen, Germany, (3) Fogra, Munich, Germany

Abstract

In the graphic arts industry, there is a need to convert colorimetric readings taken on one backing (usually white) to values that would have been measured with a different backing (usually black). We describe and compare different models for such a conversion. Starting from published models using linear scaling, we developed a new nonlinear model for a strongly scattering substrate. Another new model was derived from the Clapper-Yule model, which includes effects of internal reflectances. All these models are applicable in both the spectral and the tristimulus domain.

For calibration, we used measurements of the bare substrate on both backings. We intentionally make only use of the measured spectral or XYZ values, and do not require knowledge of the nominal CMYK values. This is particularly useful for arbitrary patches measured with a stand-alone measurement device. The test data sets consisted of a large set of test prints, originating from digital or conventional printing processes, and covering typical ranges of mass per area. Both new models outperformed linear regression models and the spectral versions always yielded better results than their corresponding versions in tristimulus space.

Introduction

In the graphic arts industry, there are many choices allowed when making spectral measurements. ISO 13655 ('Graphic technology – Spectral measurement and colorimetric computation for graphic arts images') has been recently revised in order to address various parameters. In particular, it contains requirements for both black and white backing material. Which backing is used depends on the application.

Nowadays, contract proofs are mostly created on a more or less opaque inkjet paper with a dedicated ink receiving layer, and not on the intended production stock, which is usually much less opaque. Therefore, a contract proof matching a print on white backing won't match anymore if both are placed over black backing.

An ideal solution would be the usage of the same backing material throughout the workflow. However, process control requires black backing, but prepress agencies need white backing. On the one hand, black backing minimizes the impact of back printing, the variability due to translucency effects, and prevents influence of contamination or dirt. On the other hand, white backing makes the printed product look more colourful and vibrant, and therefore sells better. Secondly, ICC-profiles based on characterization data on white backing usually result in better separation results. For these and more reasons, typical characterization data such as FOGRA39 (representing offset printing according to ISO 12647-2, gloss or matt coated stock, screen ruling of 60 lines/cm) are made on white backing.

A conversion between white and black backing is strongly demanded especially by the printers who currently have to rely on proprietary means to correct the white backing proof readings in order to achieve black backing aim values for the production

run. This means, that we model a scattering substrate in form of a laterally infinite layer partly covered with a layer of colorants, e.g. a paper printed on in halftoning technique.

In the literature, we find halftone models from Neugebauer [1], [2], Yule and Nielsen [3], Clapper and Yule [4]. All of these models predict the effect of a halftone print on the reflectance factor of a substrate with *constant* backing. For solid ink layers, the model from Kubelka and Munk [5] and its recent extensions by Yang et al. [6] would be applicable to model the covering of the backing by a scattering and absorbing layer. But none of these classical models covers both aspects, the modeling of halftone prints and the influence of backing. A comprehensive model by Mourad [7] would require patch measurements in four configurations including transmission for calibration. McDowell et al. [8] proposed a model based on tristimulus values specifically for our purpose.

In this paper, different models will be compared and tested by means of their accuracy of converting spectral or colorimetric data measured with one backing to the values that would have been measured with a different backing.

We first present the models in [8] and propose an extension of them. We then derive a second model from the ideas of Clapper and Yule [4] to finally compare performance on data from a variety of printing processes on substrates of different thicknesses.

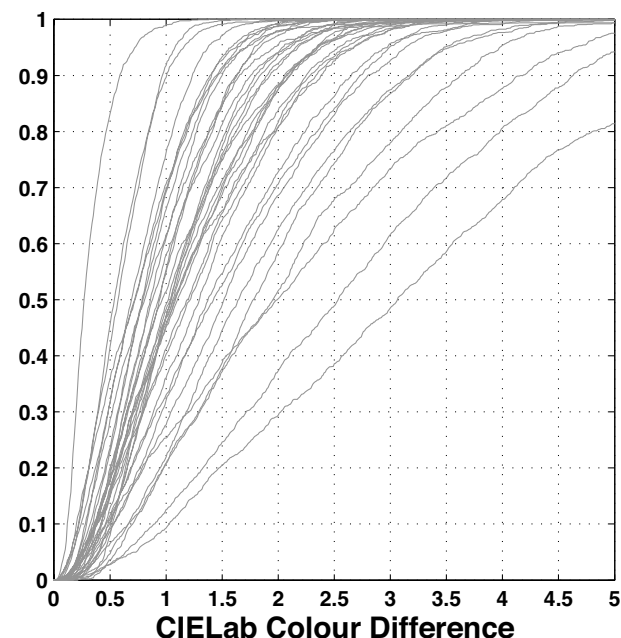


Figure 1. Cumulative distributions of colour differences due to change of backing. Each gray line stands for one of 35 characterization targets measured.

Modeling

Before we start modeling, we will have a look at the situation we are modeling. We will use our models with 35 data sets

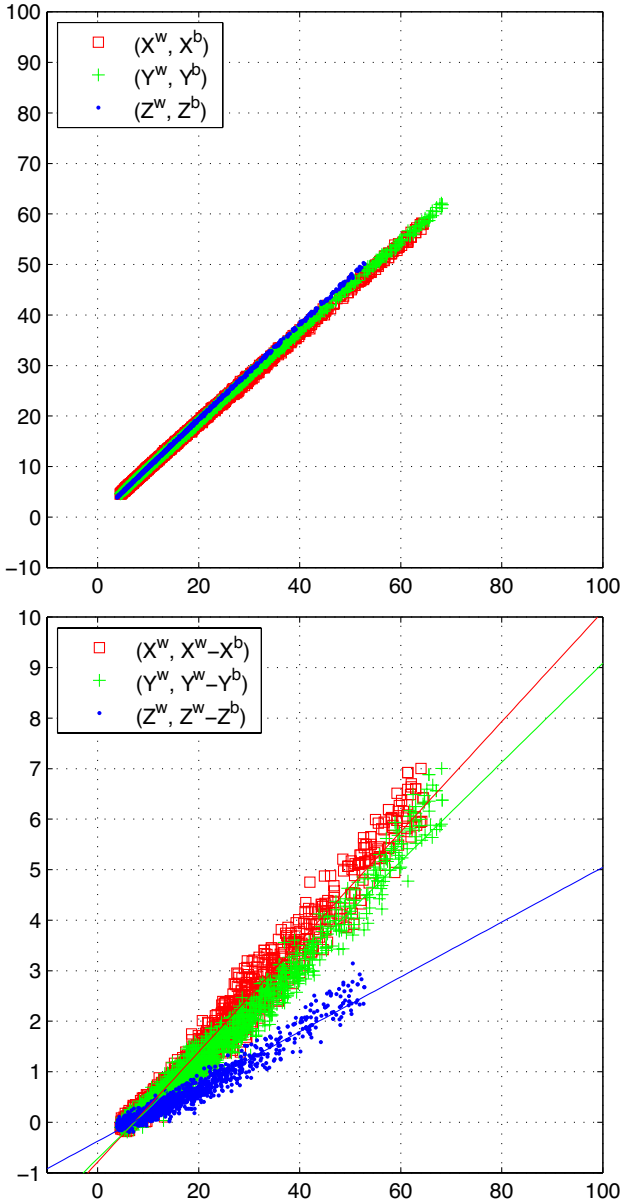


Figure 2. Linear regression model in tristimulus space seems appropriate (top). The relation from tristimulus values on white backing (X^w, Y^w, Z^w) to difference in tristimulus values ($X^w - X^b, Y^w - Y^b, Z^w - Z^b$) due to backing is almost linear (bottom).

taken from different printing processes. Each test data set corresponds to a characterization target with roughly one thousand patches (either IT8.7/3, ECI 2002, or IT8.7/4; cf. ISO 12642) measured with X-Rite Spectroscan or Barbieri SpectroLFP automated spectrophotometers, both having approximately a circular $45^\circ/0^\circ$ geometry. Readings are taken from the same sheet on black and on white backing, conforming to ISO 13655.

As illustrated in Figure 1, the median difference of measured reflectance from white to black backing is greater than $1\Delta E_{ab}$ for a majority of the patches in the average of all substrates we use for evaluation. For some substrates, the median difference is up to $3\Delta E_{ab}$. This means that using uncorrected white-backing values for production control on black backing could lead to visually different prints, regardless of the variability of the print process itself.

Linear models

If one places a black backing behind a newspaper page, the immediate observation is that everything becomes darker. Looking at XYZ or spectral data, we find a high correlation between corresponding white and black backing values. Therefore a linear correction function is a reasonable first approach. In fact, a linear scaling of spectral values was proposed by Hans Ott in 2003 according to [8]:

$$\beta_t^b = (\beta_s^b / \beta_s^w) \beta_t^w \quad (1)$$

Here, and throughout the paper, β denotes either a reflectance factor relative to a perfectly white diffuser, or, for a colorimetric context, one of the tristimulus values X, Y, or Z.¹ We use subscript t for tint to denote data of a printed patch, subscript s for bare substrate data; superscripts w and b denote measurements on white and black backing, respectively. See also Tab. 4 in the Appendix for a glossary of used symbols.

Thus, the Ott model uses the darkening of the unprinted substrate β_s^b / β_s^w as a correction factor. The McDowell et al. tristimulus model [8] adds an offset β_{min} because they observed that

‘At the lowest value of each tristimulus value, the delta between measurements made over the two backings is at or near zero.’

They give an example for newsprint paper, where the darkest patches exhibit no change from white to black backing. The Ott model would still scale those rather light blacks down.

In our notation, the tristimulus model reads

$$\beta_t^b = \beta_t^w - (\beta_s^w - \beta_s^b) \cdot \frac{\beta_t^w - \beta_{min}}{\beta_s^w - \beta_{min}} \quad (2)$$

The reflectance factor on black backing is calculated in eq. (2) based on the reflectance on white backing, reduced by a correction determined from the differences of the substrate reflectance on white and black backing and the minimum reflectance. If tints have a purely absorptive effect, eq. (2) expresses, that the difference of tint reflectance factors on both backings is bounded by the difference of substrate reflectance factors on both backings. Note that this model requires one measurement of β_{min} – on any backing, since it is assumed that at β_{min} there will be no difference between backings anyway. They suggest to use a 4-colour solid patch (100% tone value of C, M, Y, and K) to obtain this minimum value. This can be a problem because such a patch is not generally available. In our evaluation, we have alternatively tried to replace it by a solid black patch, which can be found on most control strips. We also tried a spectral version of eq. (2), despite that it was explicitly termed a ‘tristimulus correction method.’

Decomposing light paths

We will first give an alternative, more general motivation of eq. (2). Our basic idea is to model two separate flows contributing to the reflected light, the one reaching the backside, the other reflected before hitting the backside and therefore independent of the backing.

Let r be the part of reemerging incident light that never reaches the backside of the substrate. We model the passage of light through the colorant layer by the functions $t_r(\lambda)$ for r and $t_b(\lambda)$ for $(1 - r)$ respectively. The reflectance factor of a printed

¹Although we are working with spectral or colorimetric data, we mostly omit such indices for notational simplicity.

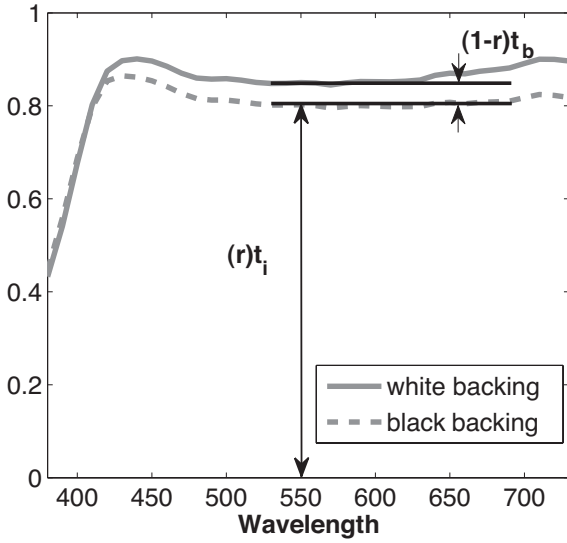


Figure 3. An example of bare substrate reflectance factors relative to absolute white, illustrating eq. 3 and eq. 4. We show the situation at $\lambda = 550$ nm, but β_s , r , t_b and t_i depend on wavelength resp. on tristimulus component.

patch on white backing β_i^w relative to absolute white, is then modeled as:

$$\beta_i^w = rt_i + (1-r)t_b, \quad (3)$$

while β_i^b , the reflectance coefficient over a black trap, should satisfy:

$$\beta_i^b = rt_i. \quad (4)$$

An example is given in Fig. 3. The parts t_i and t_b are different for each colorant layer. Generally, t_b will be $< t_i$. Since scattering is assumed to take place in the substrate only, r depends only on the substrate.

We will derive the approach of [8] from the difference between black and white backing,

$$\beta_i^w - \beta_i^b = (1-r)t_b. \quad (5)$$

Eq. (3) and (4) are also valid for the bare substrate, for which we assume $t_b = \beta_s^w$. This also implies $t_i = \beta_s^w$, so this assumption means that there is no difference for both paths on a white backing, respectively r is determined by it.

Then $(1-r)$ can be estimated from eq. (5) by the difference of the bare substrate reflectance on white backing and on black backing:

$$1-r = (\beta_s^w - \beta_s^b) / \beta_s^w \quad (6)$$

Solving eq. (5) for β_i^b results in:

$$\beta_i^b = \beta_i^w - (1-r)t_b. \quad (7)$$

Plugging our estimation of $1-r$ in eq. (7), we get an estimation of the reflectance factor on black backing:

$$\beta_i^b = \beta_i^w - (\beta_s^w - \beta_s^b) \frac{t_b}{\beta_s^w} \quad (8)$$

This means, that the reflectance of a printed sheet on black backing is modeled as the reflectance on white backing reduced by

a fraction of the difference of the bare paper measured on both backings. This fraction will be small if the colorant is highly absorbing at the respective wavelength (when t_b and t_i are small).

Note that eq. (8) still contains t_b , which must be estimated. As can be seen from eq. (2), the tristimulus model uses

$$\frac{t_b}{\beta_s^w} = \frac{\beta_i^w - \beta_{min}}{\beta_s^w - \beta_{min}}$$

However, this ignores correlations of point of entry and exit of light, which we are going to address now.

Correlation of incident and re-emitted light

In order to study the correlation of incident and re-emitted light for t_i and t_b respectively, we use a Monte Carlo simulation to calculate the point spread function (PSF) of scattered light in white paper similar to the simulation in Jenny et al. [9]. We assume isotropic scattering with a scattering length of 0.02 mm and a homogeneous paper with thickness of 0.1 mm. In Figure 4, we show the PSF of t_i and t_b in comparison with the dimensions of a typical printing raster. We scale the t_b -curve for better visibility, so peak-width relative to raster is comparable, although areas under curves are not the same.

Note that the PSF of t_i has a shape quite different from a normal distribution. It has a sharp peak at zero and broad tails on both sides. Thus, for a comparison of the two curves, we do not use their widths at half maximum. A better measure for comparison is the radius R of the circle which encloses the area, in which a defined percentage (we use 50%) of the light has re-emerged. This radius was computed as $R_i = 0.025$ mm for the PSF of t_i , and $R_b = 0.14$ mm for the PSF of t_b . R_b is in the order of one to two times the paper thickness, and very broad compared to the raster dimension. As a consequence, we may safely assume that incident and re-emitted light are uncorrelated for t_b .

For the light scattered from the bulk (t_i), the point spread function is narrow compared to the raster dimension. Correlation of incident and re-emitted light is quite strong, but far from perfect. The deviation from complete correlation, known to be the cause of optical dot gain, is not negligible and depends on the raster type and screen ruling.

Modeling the colorant layer

Based on the different PSF for t_i and t_b we want to find a better estimate of $t_b(\lambda)$ in eq. (8). We may assume it is in the range of $[0, \beta_s^w]$ to model purely absorbing tints. We reduce the spatial distribution of colorants as in the Neugebauer model to p , the fraction of the surface covered by colorants on the side of the light source. Let $q = 1 - p$ be the uncovered surface fraction and T denotes the absorption of light by a single passage of the colorant layer. Then, $\tau_u = (pT_i + qT_s)^2$ models the case where the location of incident and remitted passage are uncorrelated, while $\tau_c = (pT_i^2 + qT_s^2)$ is equivalent to the case where the locations of both passages are perfectly correlated, both ignoring internal reflections. For the broad backing-dependent function t_b we assume completely uncorrelated passages τ_u :

$$t_b = (pT_i + qT_s)^2. \quad (9)$$

The sharp backing-independent function t_i should be at least partly correlated. Therefore we need a blend of τ_c and τ_u . Instead of a weighted average, we follow Yule and Nielsen and use an exponent n , the Yule-Nielsen factor, as in

$$\beta = (p\beta_i^{\frac{1}{n}} + q\beta_s^{\frac{1}{n}})^n \quad (10)$$

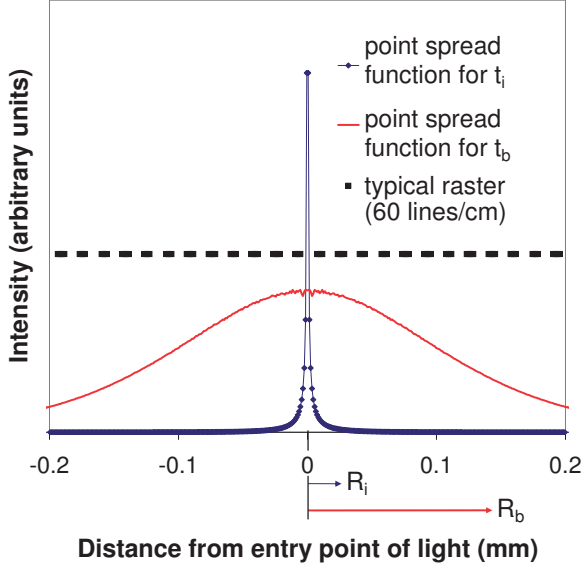


Figure 4. Simulated point spread functions of t_i and t_b in comparison with the dimensions of a typical printing raster.

Yule and Nielsen justify the replacement of 2 by n as follows [3]:

‘This equation is not rigorously true for several reasons. Surface reflection always plays a part; the internal reflections affect the result; the paper does not completely diffuse the dot pattern; and it is not certain that the small dots carry as heavy a layer of ink as the solid, or that it is uniform over the area of the dot.’

Following this argumentation, we can model the backing-independent function by substituting $n = 2^{1-\varepsilon}$ and $\beta_* = T_*^2$, $*$ $\in \{t, s\}$ in the Yule-Nielsen equation (10):

$$t_i = (p(T_i^2)^{2\varepsilon-1} + q(T_s^2)^{2\varepsilon-1})^{2^{1-\varepsilon}} = (pT_i^{2\varepsilon} + qT_s^{2\varepsilon})^{2^{1-\varepsilon}}, \quad (11)$$

where $\varepsilon = \text{const} \in [0, 1]$ is the degree of correlation. The substitution of T_*^2 stems from β_* being the solid tone or substrate reflectance factor in the Yule-Nielsen equation, where $p = 1$, respectively $q = 1$ apply, hence $\tau_c = \tau_u = T_*^2$.

Depending on T , p , and ε , equations (9) and (11) define a family of curves. Let us have a look at two corner cases: a completely absorbing tint at different levels of area coverage first, and after that, a solid colorant layer with T varying from zero to β_s^w .

We fix $T_t = 0$, $T_s = \beta_s^w$ for the first case. Then, the equations (9) and (11) can be solved for q , resulting in

$$q = (t_i)^{\frac{1}{2^{1-\varepsilon}}} (\beta_s^w)^{-2\varepsilon} = (t_b)^{\frac{1}{2}} (\beta_s^w)^{-1}. \quad (12)$$

This means, that for $T_t = 0$, $T_s = \beta_s^w$ we obtain a power law,

$$t_b \propto t_i^\gamma \quad (13)$$

with $\gamma = 2/2^{1-\varepsilon} = 2^\varepsilon \in [1, 2]$.

In the other corner case of solid patches ($p = 1$) and varying T , we get from eq. (9) and (11):

$$t_b/t_i = T_t^2 / (T_t^{2\varepsilon})^{2^{1-\varepsilon}} = \text{const}, \quad (14)$$

a linear relation with $\gamma = 1$ (actually $t_b = t_i$).

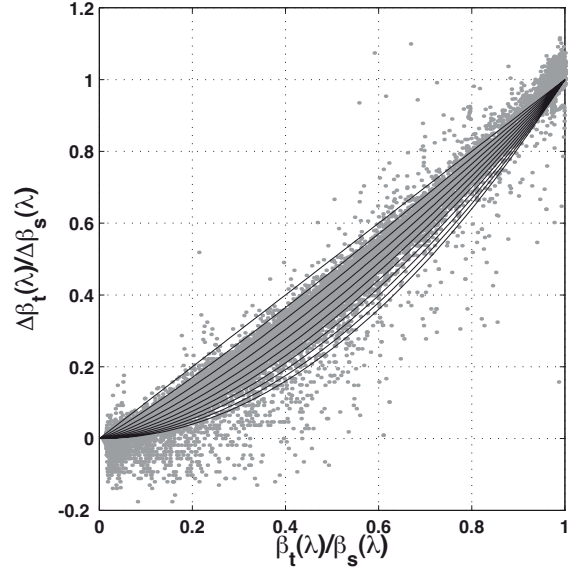


Figure 5. Relation of reflectance factor of tone (β_t^w) on white backing to the difference in reflectance factor due to backing. We normalize data with substrate reflectance factor (β_s^w) and substrate reflectance factor difference respectively. Data are in the wavelength range of 420-730 nm. The lines show the model of eq. (15), $\gamma \in [1, 2]$.

A new regression model: ‘gamma’ model

We expect from the ideas in the previous section, that the relation between the whole reflectance and the reflectance difference due to backing would be between linear and parabolic. Indeed, we do observe a monotone, nonlinear relationship between measured β_t^w and $\beta_t^w - \beta_t^b$ at the same wavelength, data scattering between a straight line and a parabola (Fig. 5).

So we conclude that data can be approximated by:

$$\beta_t^b = \beta_t^w - (\beta_s^w - \beta_s^b) \left(\frac{\beta_t^w}{\beta_s^w} \right)^\gamma, \quad (15)$$

which is a transformation of eq. (8). The right hand term τ^γ replaces t_b/β_s^w , describing the effectivity of the tint layer as in $\beta_t^w = \tau\beta_s^w$. The exponent γ expresses a relation between the effect of the tint layer on the whole reflectance and its effect on the part of the reflectance depending on the difference due to backing. For $\gamma = 1$, eq. (15) is reduced to eq. (1), Ott’s model.

To calculate white backing values from black backing with the gamma model, we use:

$$\beta_t^w = \beta_t^b + (\beta_s^w - \beta_s^b) \left(\frac{\beta_t^b}{\beta_s^b} \right)^\gamma. \quad (16)$$

Internal reflections model

Clapper and Yule [4] model the surface and internal reflections in an infinite series of passages and a surface reflectance term sk . Their model can, in our terms, be written as:

$$\beta_t^* = sk + (1-s) \frac{(1-\rho)r_*\tau_u}{1-\rho r_*\tau_c}, \quad (17)$$

where s is the surface reflectance factor, k the fraction of s captured by the instrument, ρ the diffuse internal reflection factor at the substrate-air interface, and r_* is the background reflectance for the given backing. $\tau_u = (pT + q)^2$ models the uncorrelated,

$\tau_c = pT^2 + q$ models the correlated passage through the transparent colorant layer.

The Clapper-Yule model is a six parameter model (s, k, r, ρ, p, T), where parameter r should cover all effects due to absorption in the substrate and effects of the substrate-backing interface, as they say in [4]:

‘The paper itself may not be perfectly white, so that some of the light is absorbed or transmitted by the paper. The remainder (a fraction r of the irradiance in the paper) is reversed in direction and attempts to emerge from the paper.’

We use their original values, which correspond to a refractive index of 1.5 for ink and paper, and set the specular reflectance $s = 0.04$ and the diffuse internal reflection factor to $\rho = 0.6$. We have confirmed that the latter value is indeed optimal for our data sets (not shown). The instrument factor k is small due to the directional geometry used in our measurements (see below), and we set $sk = 0$.

For convenience, we introduce the residual reflectance $\tilde{\beta} = (\beta - sk)/(1 - s)$. Then we solve eq. (17) for the substrate parameter r on both backings, setting $p = 0$ to model a measurement of bare substrate:

$$r_* = \frac{\tilde{\beta}_s^*}{1 - \rho(1 - \tilde{\beta}_s^*)} \quad (18)$$

Now that we have estimated r_w and r_b , we solve eq. (17) for the tint parameter T , here on backing w . To apply the Clapper-Yule model without using real ink area coverages, we treat the CMYK halftone patches as if they consisted of a single homogeneous ink layer, hence setting $p = 1$:

$$T^2 = \frac{\tilde{\beta}_t^w / r_w}{1 - \rho(1 - \tilde{\beta}_t^w)} \quad (19)$$

We assume that T , being an ink layer property, is the same for both backings. Therefore we can use eq. (17) with $p = 1$, T , and the other background reflectance r_b to estimate

$$\beta_t^b = sk + (1 - s) \frac{(1 - \rho)r_b T^2}{1 - \rho r_b T^2} \quad (20)$$

(and vice versa, if we want to predict β_t^w from β_t^b). If we write eq. (20) as a function of $\tilde{\beta}$, a non-linear, monotonic relationship between $\tilde{\beta}_s^w$ and $\tilde{\beta}_s^b - \beta_s^b$ can be shown with this internal reflections model as well. The equation then reads, after some transformations:

$$\tilde{\beta}_t^b = \frac{\tilde{\beta}_t^w \frac{\tilde{\beta}_s^b}{\tilde{\beta}_s^w} (\rho \tilde{\beta}_s^w + (1 - \rho))}{\rho \tilde{\beta}_t^w (1 - \frac{\tilde{\beta}_s^b}{\tilde{\beta}_s^w}) + \rho \tilde{\beta}_s^b + (1 - \rho)} \quad (21)$$

This model (21) also simplifies to Ott’s model (1) for $\rho = 0$ and $s = 0$ (i. e., $\tilde{\beta} = \beta$).

Model evaluation

While the models can be used in both directions, we focus on the conversion from white backing data to black backing (the prediction of black backing data). CIELAB values are calculated from measured data and model output using CIE Standard Illuminant D50 and the CIE 1931 Standard 2° Observer.

We evaluated our models with data taken from different printing processes, and compared our models to the uncorrected

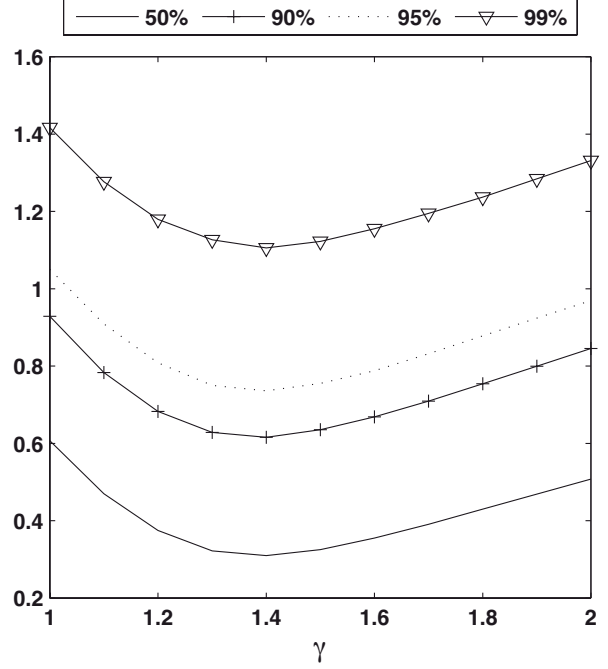


Figure 6. Quantiles of the cumulative error distribution of the model in eq. (15) with varying γ . Vertical scale in ΔE_{ab} units. $\gamma = 1.4$ is optimal.

use of measurements on one backing, and to the two linear models from [8]. Results are given as cumulative distributions of the prediction error in ΔE_{ab} (shown in Fig. 7 and 8, and their quantiles in Tab. 1 and 2). The raw differences are mostly smaller than $5\Delta E_{ab}$, so CIELAB is an appropriate space for evaluation.

The test data sets are part of Fogra’s characterization data repository,² where each set corresponds to a characterization target with typically 1500 patches, measured once on black, once on white backing, as already mentioned in the introduction.

Measurements have been conducted in dry state without a polarization filter. A subset has also been subsequently measured with a polarization filter. We will discuss the influence of filters on the values measured and on the performance of the models in the next section.

For the gamma regression model, the value of γ had to be determined first. Over all data sets, $\gamma = 1.4$ fits well, as illustrated in Fig. 6. The internal reflections model was used with standard parameters $\rho = 0.6$ and $s = 0.04$. Similar to γ , we have confirmed that $\rho = 0.6$ is indeed an optimal choice (data not shown).

The models can only be as precise as the measurements. We have estimated a lower bound for practical measurement error by measuring an IT8/7.4 target with randomized patch order and patch size > 6 mm on glossy offset stock. We have taken two passes on the same day on white backing with an X-Rite Spectroscan table with no filters equipped (M0, see below). For each patch, data were averaged from three consecutive readings. The same procedure was repeated on black backing with the same instrument. This resulted in two measurement error distributions, once for white and black backing respectively. The measurement error distribution on white backing determined this way had a 50 % quantile of $0.13\Delta E_{ab}$ and a 90 % quantile of $0.25\Delta E_{ab}$. The measurement error distribution on black backing had a 50 % quantile of $0.09\Delta E_{ab}$ and a 90 % quantile of $0.18\Delta E_{ab}$.

²<http://forschung.fogra.org/index.php?menuid=159&getlang=en>

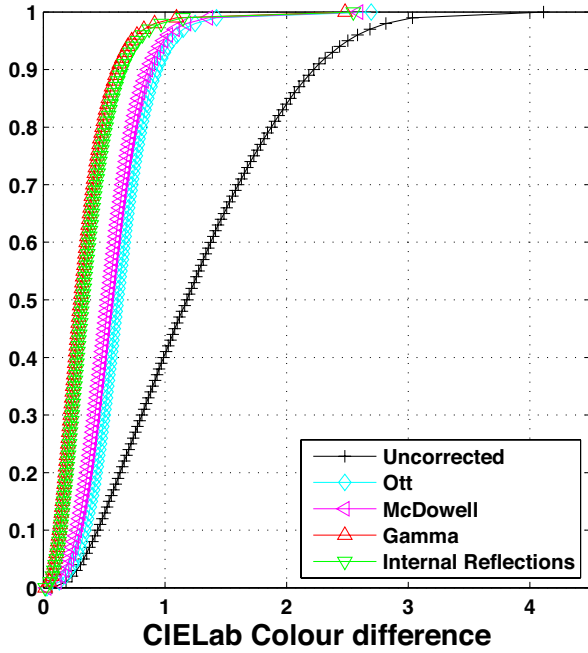


Figure 7. Cumulative error distributions of predictions by different models. Measurements on white backing were used to predict black backing values, using spectral data. Error was measured in ΔE_{ab} units.

Discussion

All models presented in this paper perform better than no correction at all. The predictions using spectral data are generally more accurate than the ones from tristimulus values. For comparison, we just show the tristimulus-based results for the McDowell model, denoted ‘(XYZ, min)’.

We have shown that our models, both the gamma regression model and the internal reflections model, contain the Ott model as a corner case ($\gamma = 1$, resp. $s, \rho \rightarrow 0$). Hence it is not surprising that the Ott model is outperformed by both.

We have argued that the linear regression of the tristimulus model in [8] can be improved by explicitly modeling the part of light reflected by the backing and accounting for an appropriate point spread function. The resulting regression curve fits the data better than both linear models.

The approach based on internal reflections yields results very similar to the gamma regression model. As Hébert and Hersch pointed out in [10], the relationship from layer transmittance t_λ (as they call it) to reflectance is not linear in the Clapper-Yule model. It has a shape very similar to the one described by the

Table 1. Quantiles of prediction error distributions, averaged over all targets, by different models. Measurements on white backing β_i^w were used to predict black backing values β_i^b . Error was measured in ΔE_{ab} units.

Name	50%	90%	95%	99%
Uncorrected (just using β_i^w)	1.18	2.22	2.50	3.04
McDowell (XYZ, min)	0.55	0.93	1.07	1.47
Ott (spectral)	0.61	0.93	1.06	1.42
McDowell (spectral, min)	0.53	0.86	0.99	1.35
Gamma Regression	0.31	0.61	0.73	1.10
Gamma (min corrected)	0.31	0.62	0.73	1.09
Internal Reflections	0.33	0.65	0.77	1.15
Internal Reflections (s=0)	0.33	0.65	0.78	1.15

gamma model (see [10], Figure 15).

In the case of linear models, correcting β_{min} is a good idea, as the McDowell model performs better than the Ott model for this reason. Our data shows, that the gamma regression model does not profit from subtracting the darkest spectrum from both spectra in β_t/β_s before applying the exponentiation (denoted ‘Gamma (min corrected)’ in tables 1 and 2 respectively). We attribute this to the different shape of the regression curve.

Since the internal reflections model is already considerably simplified by assuming a non-screened (non-halftoned), homogeneous colorant layer, we ask whether the small surface reflection term is important for our application. We present results for $s = 0$ which show that there is no significant difference. The non-screened approximation probably dominates the model error.

The accuracy of the tested models is virtually the same if one converts from black backing to white backing. Maximum differences are smaller than $0.04 \Delta E_{ab}$. All in all, the gamma regression model and the internal reflections model are already close to the limit of measurement uncertainty (less than a factor of 3 away from the quantile values of our optimum conditions).

Measurement condition differences

In practical colour management use cases it is often desired to convert between different measurement conditions, such as those defined in ISO 13655, namely M0, M1, M2, and M3. They differ e. g. by the level of UV excitation, the usage of polarization filters and potentially the used backing. For process control in offset printing the correlation between measurements with (M3) and without polarization filters (typically M0) is of great interest. While polarization filters suppress first surface reflectance and therefore achieve stable readings with both wet sheets directly after printing and dried sheets, measurements for final quality assessment (e.g. print compliance according to ISO 12647-2) must be made without polarization filters. We compare data from 20 targets that have been measured on both black and white backing, once without filters (M0), and once with polarization filters (M3) to remove the specular part of reflectance.

Differences due to backing are bigger with than without polarization filters. Expressed in numbers, half the patches differ by more than $1.8 \Delta E_{ab}$ due to backing when measured with M3, compared to $1.6 \Delta E_{ab}$ with M0 (Tab. 3).

The quantiles of the cumulative prediction error distribution of the models deviate less than $0.1 \Delta E_{ab}$ between M0 and M3, with the notable exception of the Ott model that consistently performed better correcting backing change under condition M3. This means, that the models presented here can convert M3 measurements as well as M0 measurements with regard to the back-

Table 2. Quantiles of prediction error distributions, averaged over all targets, by different models. Measurements on black backing β_i^b were used to predict white backing values β_i^w . Error was measured in ΔE_{ab} units.

Name	50%	90%	95%	99%
Uncorrected (just using β_i^b)	1.18	2.22	2.50	3.04
McDowell (XYZ, min)	0.56	0.94	1.09	1.49
Ott (spectral)	0.62	0.95	1.08	1.45
McDowell (spectral, min)	0.55	0.88	1.01	1.38
Gamma Regression	0.31	0.62	0.74	1.12
Gamma (min corrected)	0.32	0.62	0.74	1.11
Internal Reflections	0.33	0.66	0.79	1.17
Internal Reflections (s=0)	0.33	0.66	0.79	1.17

Table 3. Averaged quantiles of error distributions of predictions of β_t^b from β_t^w under two measurement conditions (20 targets, total of 27868 patches). Error was measured in ΔE_{ab} units. M0: no filter; M3: polarization filters.

Name	50%	90%	95%	99%
Uncorrected (using β_t^w), M0	1.60	3.18	3.61	4.33
Uncorrected (using β_t^w), M3	1.84	3.58	4.05	4.76
Internal Reflections (s=0), M0	0.36	0.62	0.72	1.08
Internal Reflections (s=0), M3	0.34	0.64	0.75	0.99

ing. However, the models presented here do not predict M3 measurements from M0 measurements.

For reasons of usability in practical applications, we have tested the models with fixed parameters γ, ρ, k or s . Variation of these parameters might yield more accurate results for particular substrates.

Conclusions

We have proposed two models to predict the influence of backing on the reflectance factor of colour patches on a particular substrate. The reflectance factor of substrate and patches are measured on one backing and are then used to predict values on the other backing by measuring only the substrate reflectance factor on this second backing. Both models fulfill this requirement of usability.

The new gamma regression model as well as an application of the ideas of Clapper and Yule perform better than linear models. There is no significant difference in performance between the internal reflections model and the gamma regression model.

The developed models are currently subject for process control implementation for the printing industry. However, further aspects such as wet-dry-behaviour, lack of inter-instrument agreement, and problems with regard to the usage of optical brightener agents (OBA) have also to be taken into account. Closer analysis with regard to CMYK values of the individual patches and correlations to point spread function or angular distribution of light may be subject of future work as well.

Acknowledgment

Part of this project was funded by the Federal Ministry of Economics and Technology to support the "Industrielle Gemeinschaftsforschung (IGF)" via the German Federation of Industrial Cooperative Research Associations (AiF).

References

- [1] H. Neugebauer. Die theoretischen Grundlagen des Mehrfarbendruckes. *Z. Wiss. Photogr.*, 36:73–89, 1937.
- [2] H. Neugebauer. The theoretical basis of multicolor letterpress printing (translated by D. Wyble and A. Kraushaar). *Color Res. Appl.*, 30:322–331, 2005.
- [3] J. A. C. Yule and W. J. Neilsen [sic]. The penetration of light into paper and its effect on halftone reproduction. *Proc. TAGA*, pages 65–75, 1951.
- [4] F. R. Clapper and J. A. C. Yule. The effect of multiple internal reflections on the densities of half-tone prints on paper. *Journal of the Optical Society of America*, 43(7):600–603, 1953.
- [5] Paul Kubelka and Franz Munk. Ein Beitrag zur Optik von Farbanstrichen. *Zeitschrift für technische Physik*, pages 593–601, 1931.
- [6] L. Yang and S. Miclavcic. Revised Kubelka Munk Theory III. A general theory of light propagation in scattering and absorptive me-

dia. *Journal of the Optical Society of America*, 22(9):1866–1872, 2005.

- [7] Safer Mourad. Improved calibration of optical characteristics of paper by an adapted paper-MTF model. *Journal of Imaging Science and Technology*, 51:283–191, 2007.
- [8] David Q. McDowell, Robert Chung, and Lingjun Kong. Correcting measured colorimetric data for differences in backing material. In *TAGA Proceedings*, pages 302–309, 2005.
- [9] Patrick Jenny, Safer Mourad, Tobias Stamm, and Klaus Simon. Computing light statistics in heterogeneous media based on a mass weighed probability density function method. *Journal of the Optical Society of America, A*, 24(8):2206–2219, 2007.
- [10] M. Hébert and R. D. Hersch. Classical print reflection models: a radiometric approach. *Journal of Imaging Science and Technology*, 48(4):363–74, 2004.

Author Biography

M. Scheller Lichtenauer studied Computer Science at ETH Zurich, where he received his Master of Science in 2008. He then joined the Media Technology Lab at EMPA to develop colour prediction models for print. He as well works on imaging and image analysis in research.

Hanno Hoffstadt received his Ph. D. in biophysics from the University of Gießen, Germany. Since 1998 he has worked in prepress, printing and colour management. In 2006, he joined GMG as a colour scientist and is responsible for research on spectral methods.

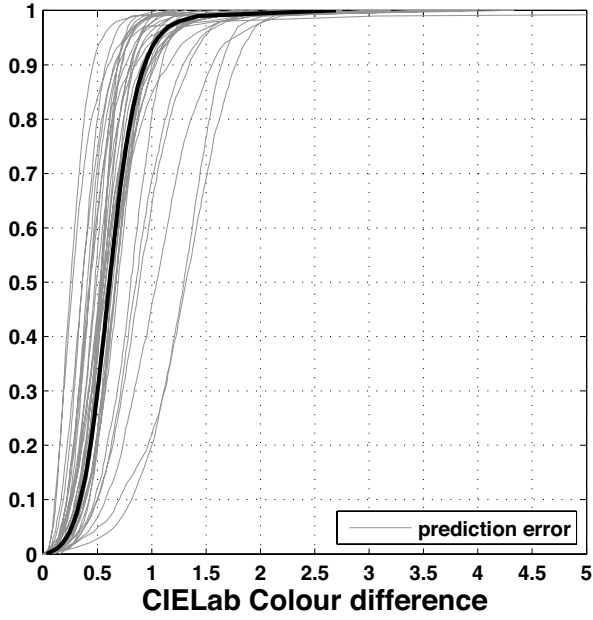
Andreas Kraushaar is head of the prepress division at Fogra, Munich. He joined Fogra in 2001 and is responsible for colour management, preflighting production data, and contract proofing. He received a master degree in media technology from the Technical University Ilmenau and is currently a candidate for a doctoral degree from Aachen University.

Berthold Oberhollenzer received a diploma in print and media technology from the Munich University of Applied Science prior to join Fogra in 2009, where he investigates methods to transfer target values from proof to print.

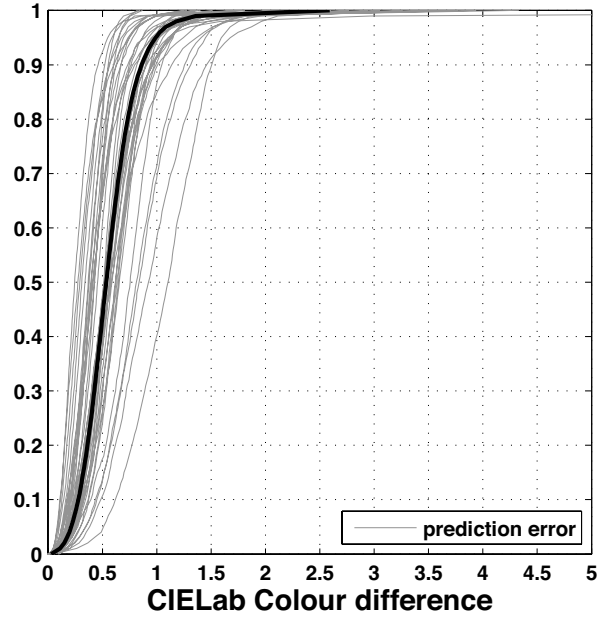
Peter Zolliker studied Physics at ETH Zurich and received his Ph. D. in Crystallography from the University of Geneva in 1987. After his postdoc position at the Brookhaven National Laboratory in New York, he joined Gretag Imaging in 1988. Since 2003 he is working at EMPA where he is engaged in color management and statistical analysis.

Table 4. Glossary of parameters and symbols.

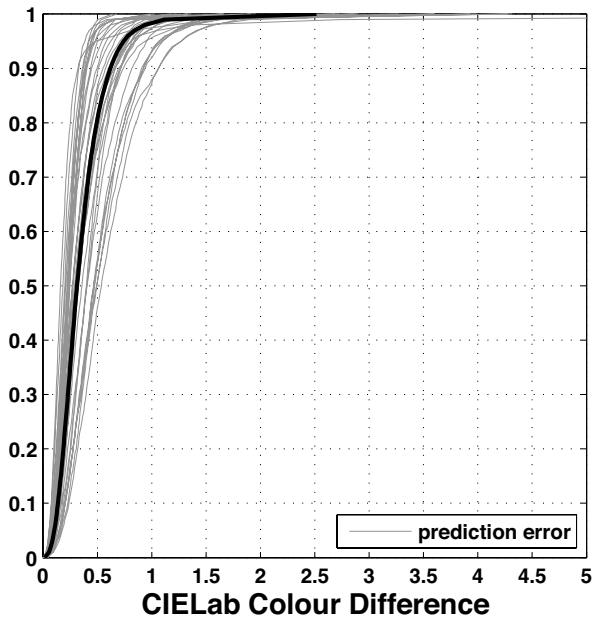
X^w, Y^w, Z^w	Tristimulus values on white backing
X^b, Y^b, Z^b	Tristimulus values on black backing
β_s^w	Reflectance factor of substrate on white backing
β_s^b	Reflectance factor of substrate on black backing
β_t^w	Reflectance factor of patch on white backing
β_t^b	Reflectance factor of patch on black backing
T	Cumulated effect of all tint layers relative to absolute white
p	Area fraction covered with any tint
q	$1 - p$, Unprinted area fraction
t_i	Effect of tints on light reflected in the bulk
t_b	Effect of tints on light reflected by the backing
τ_c	Effect of correlated entry and exit
τ_u	Effect of uncorrelated entry and exit
n	Yule-Nielsen factor
ϵ	Effective degree of correlation
γ	Exponential parameter in regression model
ρ	Internal reflectance coefficient
s	Surface reflectance in internal reflectance model
k	Geometrical correction in internal reflectance model



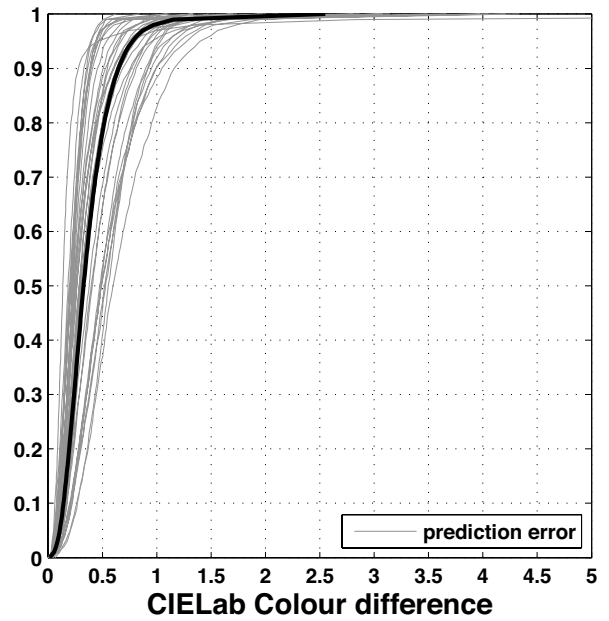
(a) Ott model, eq. (1)



(b) Tristimulus model, eq. (2)



(c) Gamma model with $\gamma = 1.4$, eq. (15)



(d) Clapper-Yule model with solid approximation, eq. (20)

Figure 8. Cumulative distribution of the prediction error by model and target. Each gray line stands for one of the targets evaluated. Each target contained several hundreds of colour patches measured. Thick black lines: quantiles averaged over all targets.